

CHARA Array adaptive optics: complex operational software and performance

Narsireddy Anugu^{a,*}, Theo ten Brummelaar^b, Nils H. Turner^b, Matthew D. Anderson^b, Jean-Baptiste Le Bouquin^c, Judit Sturmman^b, Laszlo Sturmman^b, Chris Farrington^b, Norm Vargas^b, Olli Majoinen^b, Michael J. Ireland^d, John D. Monnier^e, Denis Mourard^f, Gail Schaefer^b, Douglas R. Gies^b, Stephen T. Ridgway^g, Stefan Kraus^h, Cyril Petitⁱ, Michel Tallon^f, Caroline B. Limⁱ, and Philippe Berio^f

^aSteward Observatory, Department of Astronomy, University of Arizona, Tucson, USA

^bCHARA Array, Georgia State University, Atlanta, GA 30302, USA

^cInstitut de Planetologie et d'Astrophysique de Grenoble, Grenoble 38058, France

^dThe Australian National University, Canberra, ACT 2600 Australia

^eUniversity of Michigan, Ann Arbor, MI 48109, USA

^fUCA/OCA/CNRS, Campus Valrose, 28 avenue Valrose, 06108 Nice France

^gNOIRLab, NSF's National Optical-Infrared Astronomy Research Laboratory, 950 N. Cherry Ave., Tucson, AZ 85719, USA

^hSchool of Physics and Astronomy, University of Exeter, Exeter, Stocker Road, EX4 4QL, UK

ⁱDOTA, ONERA, Université Paris Saclay, F-91123 Palaiseau - France

ABSTRACT

The CHARA Array is the longest baseline optical interferometer in the world. Operated with natural seeing, it has delivered landmark sub-milliarcsecond results in the areas of stellar imaging, binaries, and stellar diameters. However, to achieve ambitious observations of faint targets such as young stellar objects and active galactic nuclei, higher sensitivity is required. For that purpose, adaptive optics are developed to correct atmospheric turbulence and non-common path aberrations between each telescope and the beam combiner lab. This paper describes the AO software and its integration into the CHARA system. We also report initial on-sky tests that demonstrate an increase of scientific throughput by sensitivity gain and by extending useful observing time in worse seeing conditions. Our 6 telescopes and 12 AO systems with tens of critical alignments and control loops pose challenges in operation. We describe our methods enabling a single scientist to operate the entire system.

Keywords: Long baseline interferometry, Adaptive optics, Shack-Hartmann, CHARA, Wavefront sensor, EM-CCD

1. INTRODUCTION

The CHARA Array¹⁻³ is the world longest baseline optical or near-infrared interferometer with six 1-meter diameter telescopes and baseline up to $B = 331$ m delivering sub-millisecond angular resolution (e.g., $\lambda/2B \sim 0.6$ mas at H-band). The six telescopes of the CHARA Array are arranged in a Y-shaped configuration, and they provide 15 interferometric baselines and 20 closure phases. The CHARA Array has been a very successful observatory so far by delivering landmark results in the areas of stellar imaging,^{4,5} binaries,^{6,7} expansion phase of a nova explosion,⁸ and stellar radii measurements⁹ with a sub-millisecond angular resolution. However, to achieve the challenging goals of imaging faint targets such as young stellar objects and active galactic nuclei, and measuring radii of TESS exoplanet host targets require higher instrument sensitivity.

Since obtaining the first-fringes, the beam combiner laboratory of the CHARA Array is equipped with fast tip-tilt systems,¹⁰ although the original goal was to deploy adaptive optics systems (AO) for the telescopes and

* Steward Observatory Fellow in Astronomical Instrumentation and Technology.

E-mail: nanugu@arizona.edu

in the laboratory. Since 2012, the CHARA Array adaptive optics programs are under development in the beam combiner laboratory and at the telescopes. They are developed in two phases, accommodating funding realities (PI: Theo ten Brummelaar). These adaptive systems enable higher throughput by increasing the Strehl ratio of each beam. The light collected by the telescopes is injected into single-mode fibers, is a standard practice currently in the field, for spatial filtering¹¹ before the beam combination inside a beam combiner (e.g., MIRC-X,¹²⁻¹⁴ MYSTIC¹⁵ and SPICA^{16,17}). The sensitivity of optical interferometers is an order of a magnitude lower than those in most classic telescopes is due to:

- Too many mirrors in the light path from the sky to a beam combiner, e.g., the CHARA Array contains 21 mirrors. Furthermore, telescope and instrument vibrations play a huge role.
- Non-common-path errors in an interferometer are orders of magnitude greater than those in the most telescope AO systems.
- Interferometers combine coherent light to make fringes, but because of atmospheric turbulence, only short coherent integrations are allowed – smaller than the atmospheric coherence time, typically 10-25ms.
- Atmospheric turbulence severely limits the light coupling into the single-mode fibers with a distorted point spread function.¹¹ For a pupil with a central obstruction of 25% of the pupil diameter, the expected coupling efficiency into a single-mode fiber is 0.69 times the Strehl ratio.¹⁸ To improve the instrument throughput, we need high Strehl ratio beams at the tip of single-mode fibers.

Without adaptive optics, the sensitivity of observing the faintest star with any beam combiner at the CHARA Array is lower than eight magnitudes in H or K-bands.

The CHARA Array has twelve adaptive optics systems in total :

- **Tel-AO (in Phase II)**¹⁹⁻²² Six at the telescope sites to correct the tip-tilt and high-order aberrations induced by the atmospheric turbulence. These AO systems provide high Strehl ratio beams to the vacuum tubes, which transport the light to the beam combiner lab.
- **Lab-AO (in Phase I)**^{23,24} Six at the beam combiner lab to correct significant non-common path aberrations that arose between the telescope and the beam combiner instruments. The non-common path aberrations errors are due to several hundred meters of the light path in between the telescope and the beam combiner, including several mirrors and delay lines.

The Lab-AO systems were commissioned already in Phase I²³ and are in operation since 2014 for science observations as reported in the previous SPIE proceedings.²¹⁻²⁴ The Tel-AO systems have been commissioned since 2018, in incremental steps, one telescope after another. The preliminary optical design of the Tel-AO systems is presented in 2018 SPIE proceedings.¹⁹ In this presentation, we report the software architecture, operation, and results.

A few challenges we face in the operation of the twelve adaptive optics systems are:

- **Obtain high-Strehl ratios by making a good AO correction** For this, the software development requires acquiring low-latency frames from the wavefront sensor camera, computation of slopes, computation of control matrix, correction of high-order aberrations with the ALPAO deformable mirrors (DM), and tip-tilts with the telescope M2.
- **Alignment between Tel-AO and Lab-AO** The Lab-AO is connected to the Tel-AO using a metrology system. The Lab-AO wavefront sensor (WFS) records beacon light sent from the telescope that uses a wavelength outside that of the science band of interest to measure the non-common path aberrations.¹⁹ A dichroic at the telescope reflects some visible wavelengths of starlight into the Tel-AO WFS, and it also sends the beacon light into the Lab-AO WFS. The beacon light must follow the same light path as the star. We require an automatic alignment in pupil and focus.

- Complexity in operation** Control of six telescopes and twelve adaptive optics systems by an operator is a challenge. Several Graphical User Interface (GUI)s execute the control of these systems. Each system has its own GUI, for instance, GUI for the telescope, acquisition camera, telescope tip-tilt, Tel-AO, and Lab-AO. Many GUIs invite inefficiency and error. Our challenge is to present a manageable interface for the operator. For example, the Tel-AO and Lab-AO systems alone require six monitors to fit their GUIs. For each slew to a new star target, the sequence includes the telescope pointing and tracking, star acquisition with the acquisition camera, locking the closed-loops of the tip-tilt, Tel-AO, and Lab-AO. We required an efficient software system and an integrated, stable, and easy operable GUI for each telescope to do all these steps in a small amount of time to maximize the time for the fringe finding and recording.

2. OVERVIEW OF CHARA ADAPTIVE OPTICS

Figure 1 shows the Tel-AO and Lab-AO systems as built. A brief description of the optical design of each system is followed below.

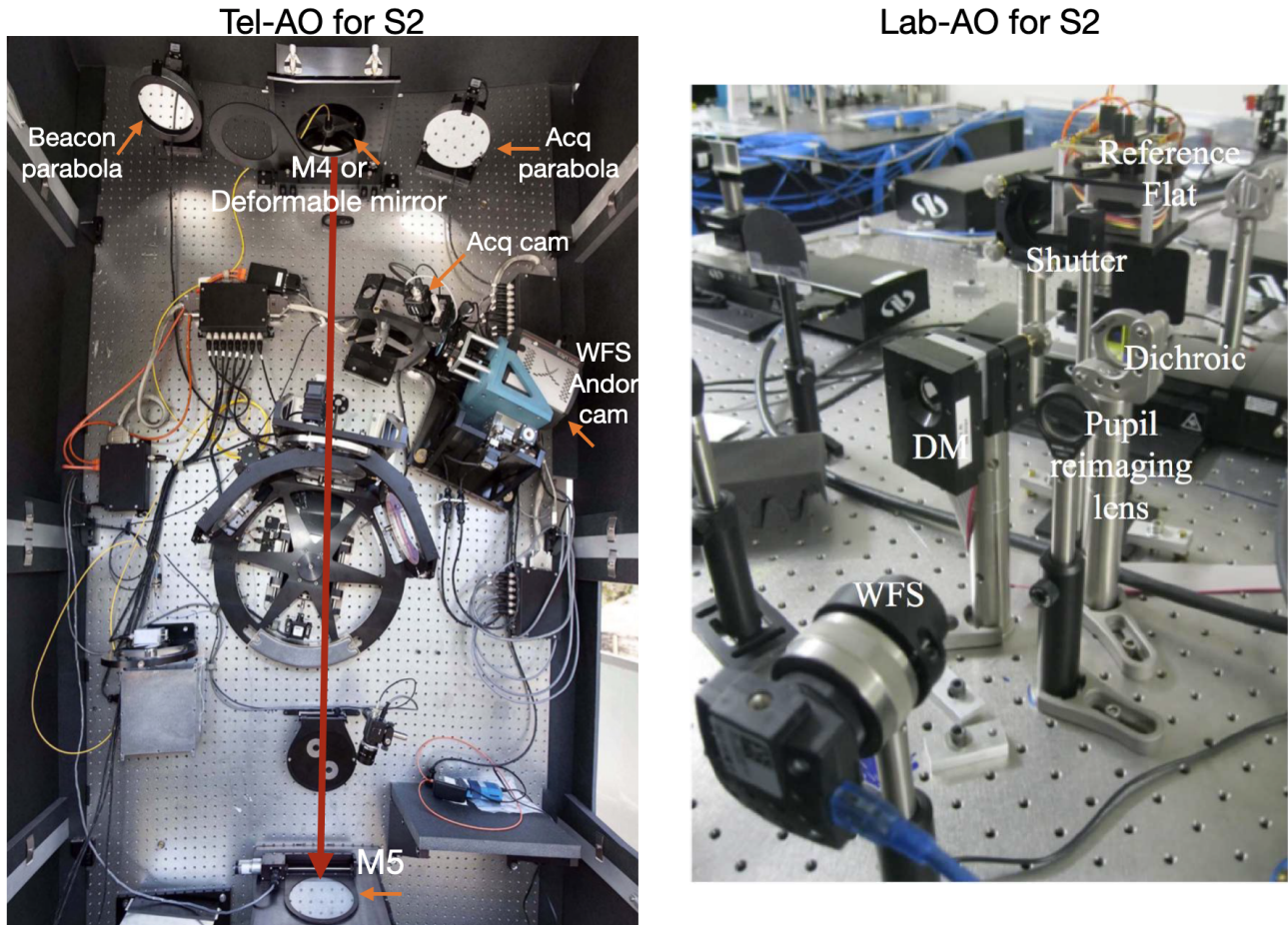


Figure 1. Photographs of the Tel-AO (left) and Lab-AO systems (right) as built.

2.1 The telescope adaptive optics system (Tel-AO)

The Tel-AO is designed to correct the atmospheric turbulence above the telescope and improve the Strehl ratio of the beams in H or higher wavelengths. Each Tel-AO system consists of (a) a 7×7 lenslet based Shack-Hartmann wavefront sensor and a 500 Hz fast frame rate and sub-electron readout noise, Andor 897 EMCCD camera²¹ and (b) an ALPAO voice-coil based deformable mirror with 61 actuators.¹⁹ The Tel-AO DMs are placed in the position of the M4 mirror to limit new reflections to the beam train. This mirror position is at 45 degrees, and

this orientation results in an ellipse pattern pupil. The DM and the Shack-Hartman match this ellipse shape. The Tel-AO has three dichroic glasses: BARE, VIS, and YSO. Based on a science requirement, an appropriate dichroic filter is chosen to maximize flux into the Tel-AO WFS. Table 1 presents the dichroic filter and their percentage of share into the Tel-AO WFS.

The expected performance of Tel-AO is (i) more than one magnitude sensitivity improvement in good seeing conditions (Fried parameter $r_0 > 15\text{cm}$ at $\lambda = 0.5\mu\text{m}$), and (ii) 1-3 magnitude sensitivity improvement for $5 < r_0 < 15\text{cm}$ and that means three times of more high quality observing time.

Table 1. Tel-AO dichroic filter selection and % light shared with the Tel-AO WFS

Dichroic glass	Share to the Tel-AO WFS
BARE	4%
VIS	20%
YSO	100%

Table 2. Deformable mirror specifications

Parameter	Tel-AO	Lab-AO
DM actuators	ALPAO 61	OKO MMDM 37
Size	18cm	15 mm
Dynamic range	$16\mu\text{m}$	$9\mu\text{m}$
Inter-actuator stroke	$4\mu\text{m}$	$0.5\mu\text{m}$
First resonance	500 Hz	-
Settling time	2ms	-
Mirror best flat	$< 30\text{ nm}$	400 nm
Optimized for H and K-bands	Spacing of sub-apertures is $\sim 14\text{cm}$ on telescope pupil $r_0 \sim 5\text{cm}$ at $0.5\mu\text{ m}$, $r_0 = 21\text{cm}$ at $1.6\mu\text{m}$	

2.2 The laboratory adaptive optics system (Lab-AO)

The Lab-AO systems are placed after the delay lines in the beam combiner laboratory and just before the beam combiner instruments.²³ The Lab-AO is intended to correct for non-common path errors in the system, which are significant as there are several hundred meters of the path in each beam, each including several mirrors and delay line carts.

To reduce the cost of the Lab-AO systems, use off-the-shelf DM (OKO MMDM with 37 actuators) and 6×6 lenslet imaged with a USB CCD camera. Since the Lab-AO uses the beacon from the telescope, there is enough light, and a high-readout noise camera is not a problem. The performance of the Lab-AO systems are not at the level of a standard adaptive optics system (see Table 2 and 3), and as it is used only for quasi-static aberrations: (i) it has a lower number of actuators, and its WFS operates at a lower speed 100Hz, and (ii) The measured wavefront errors are in a low order compared to the Tel-AO WFS estimated wavefront errors.

3. CONTROL SOFTWARE ARCHITECTURE AND DEVELOPMENT

3.1 The Tel-AO computer hardware

The computer server plays a critical role in the adaptive system’s performance. It needs to read wavefront sensor images with a low-latency and process them for wavefront slopes and compute the command matrix without much additional delay. The Tel-AO computer hardware is entirely commercial off-the-shelf (COTS), utilizing standard components. There are six computers, one for each telescope, and the fundamentals of these computers and data acquisition frame grabbers are identical, meaning they use the same motherboard, processor, and RAM. The computers’ selection is driven by low-power consumption as the WFS camera is placed inside the telescope

Table 3. Wavefront sensor specifications

Parameter	Tel-AO	Lab-AO
Lenslet sub-apertures	7×7	6×6
Effective sub-apertures	36	32
Sub-aperture field of view	6.7''	4.6''
Pixel per sub	9	5
camera window size	90×90	160×128
Frame rate	500Hz	100Hz
Sensitivity R-band	< 14 with EMCCD gain	< 4
Zernikes measured	21	21

dome. The Andor 897 EMCCD works with USB control with limited length cables. The computers are selected with the specification of Intel CPU 6 Cores with i7-8700 clock speed 3.20GHz. These computers are operated with the Ubuntu Linux low latency operating systems with kernel 4.4.0.

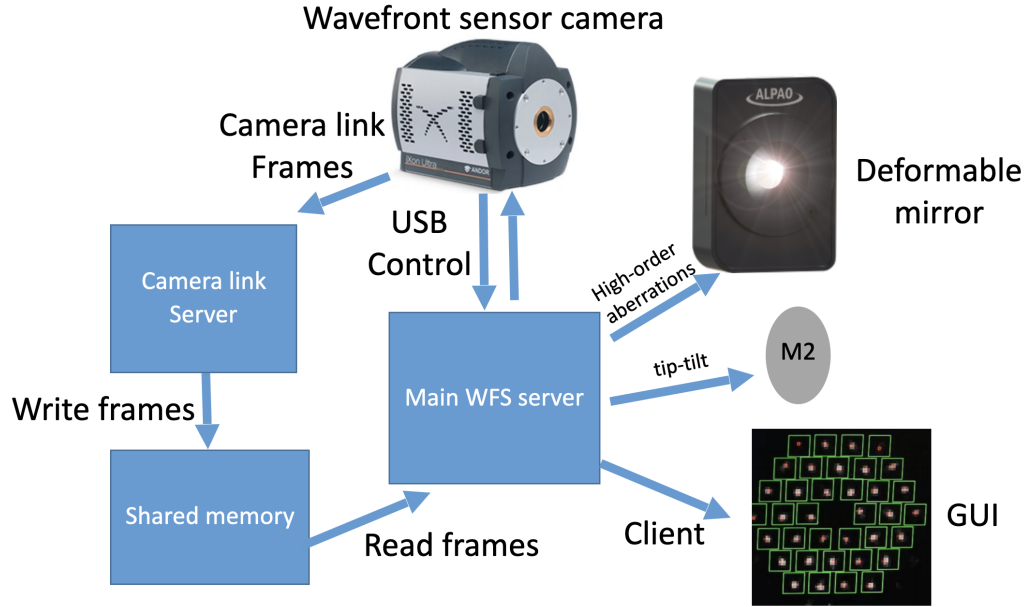


Figure 2. The Tel-AO software layout. The camera link server reads the frames from the WFS Andor EMCCD camera through BitFlow Neon frame grabber and writes them to an instrument shared memory in a circular buffer so that the main WFS main server uses them. The WFS main server reads the frames from the instrument shared memory and calculates the wavefront slopes from each new science frame. Next, the DM commands are computed by multiplying the slopes matrix with the slopes-to-actuator reconstructor matrix. The tip/tilt is computed by taking the average of slopes and then sent to telescope M2 for correction with appropriate gain. The rest higher-order corrections are sent to the ALPAO deformable mirror. The wavefront sensor images and deformable mirror shapes are sent to the client GUI for monitoring and operation.

3.2 The Tel-AO low latency software

The software development of the Tel-AO systems (see Figure 2) involves acquiring low-latency wavefront sensor images, computation of slopes,²⁵ computation of control matrix, correction with the ALPAO deformable mirrors, and telemetry data recording. Furthermore, the software handles the automated stabilization of pupil and beacon drifts. We follow a modular design, whereby multiple processes/threads interact through shared memory to process the camera data at a full-frame rate with minimum latency.

We realized the default USB-based data acquisition of the Andor camera is missing frames (see Figure 3), and as a solution, we implemented a low latency frame grabbing solution with a BitFlow Neon CLB frame grabber. Before trying BitFlow frame grabber, we tried Matrox Radiant eV-CL frame grabber, and it did not work as the Andor camera link out is non-standard in the market: base configuration, 3-tap interface, and 16-bit greyscale. We were able to find another working frame grabber, Epix, but the latency jitter was high compared to the BitFlow Neon CLB frame grabber. The frames produced by the camera are written to an instrument shared memory, and those are accessed directly by the main wavefront sensor server. The main server computes slopes from raw images, commands from slopes matrix, and controls the deformable mirror for the correction of high-order aberrations and the telescope M2 mirror for the correction tip-tilts (see Figure 2).

In Figure 3, we compare the USB based data acquisition and camera-link based data acquisition. The time difference between two consecutive frame grabs is recorded 1000 times. In a low latency situation, one expects to get one frame for each frame grab request, and the time difference between two consecutive grabs is more or less equal. In a jitter frame grabbing situation, we get more than one frame in a grab, and the time difference between two consecutive grabs is not the same (sometimes considerable big time and some less time). The USB data acquisition has many jitters in frame arrival, and the average consecutive frame arrival is for every 10ms for an integration time of 3ms. In the worst case, a USB frame grab gets eight frames in a chunk (i.e., eight frames of delay, which means a delay between consecutive frames is more significant than 24ms). In the camera-link case, there is jitter in the frame arrival but very small – average consecutive frames arrival for every 3.1ms for the integration of 3ms. Here we do not report the pure delay.

We list below the Andor functions used in our software. These were critical in getting a low-latency arrival of frames from the Andor camera; otherwise, we noticed an additional pure delay of two frames, at 2ms integration. The measure of pure delay of the WFS Andor camera is attempted by sending a series of impulse pokes on the ALPAO deformable mirror and noticing the resulting shapes on the wavefront sensor, and computing the time delay. The known deformable mirror delay is subtracted from this measurement. For a 2ms integration time, we measure 1.8ms pure delay, which is the sum of the camera frame transfer time and readout time. For comparison, this is almost similar to NAOMI,²⁶ and their reported value is 1.54ms. They use the same Andor 897 camera, but the difference of lower 0.26ms maybe due to the usage of their hard real-time operating machine for frame grabbing than our COTS machine.

```

vspeed(2)           -> 0.5 microseconds
hspeed(2)           -> 10MHz
SetFrameTransferMode(1) -> readout in Frame Transfer Mode
SetReadMode(4)      -> readout mode image
SetIsolatedCropMode(1, 90, 90, 1, 1) -> read cropped 90x90 pixels with
                                starting vertical and horizontal bins
SetIsolatedCropModeType(1) -> low latency mode saves 2 frames of delay
SetAcquisitionMode(5) -> acquisition run till abort
StartAcquisition()  -> starts the acquisition

```

The influence functions of all DM actuators were measured in a standard method using the wavefront sensor. Each actuator is "poked" and the resulting influence on the wavefront is measured. The actuator poking was done in positive and negative directions to minimize the measurement's noise by taking the average of both amplitudes. Furthermore, 100 wavefront measurements were taken for each poke to average out and reduce the noise of the WFS detector.

A challenge for telemetry data recording is management since we have twelve systems. We only save telemetry data when requested by the user as all the AO systems generate more than 1TB of data per night. An important feature of our telemetry data recording and saving is that the data is recorded into memory and saved to disk without interrupting priority tasks. The telemetry data includes time-stamped wavefront sensor images, measured slopes, aberrations, and actuator-to-slopes reconstructor matrix. This telemetry data used to estimate the performance of the AO system, and as well as it is used to correlate with science fringe data during post-processing.

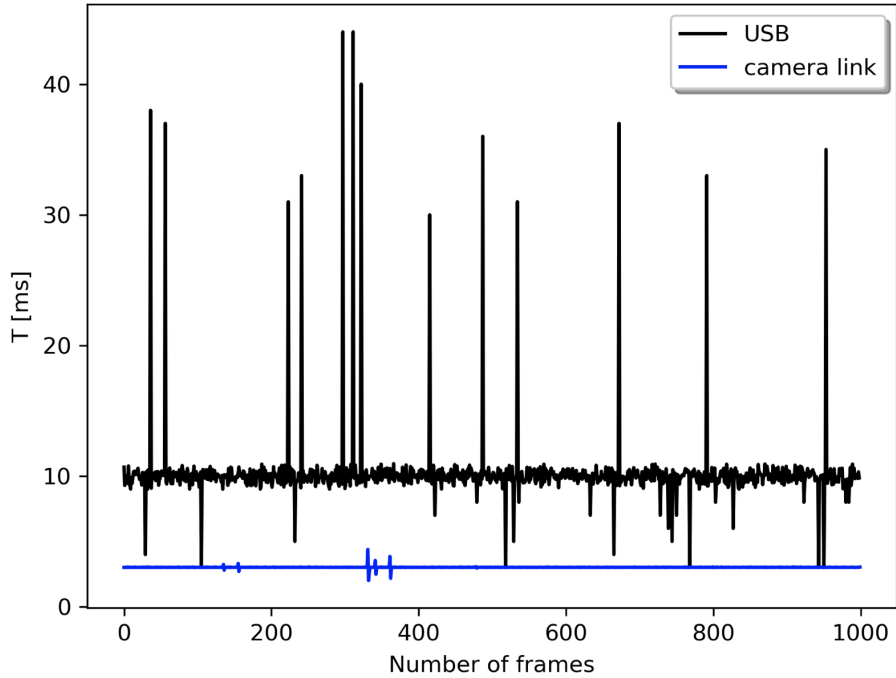


Figure 3. USB data data acquisition of frames (black color) in a comparison to the camera-link data acquisition (blue color). The integration is 3ms but the data points are the time difference between two consecutive frame grabs. The USB acquisition has a lot of jitters, in a worst-case, a grab gets 8 frames in a chunk (i.e., 8 frames of delay). In the case of camera-link, there is also jitter but very small.

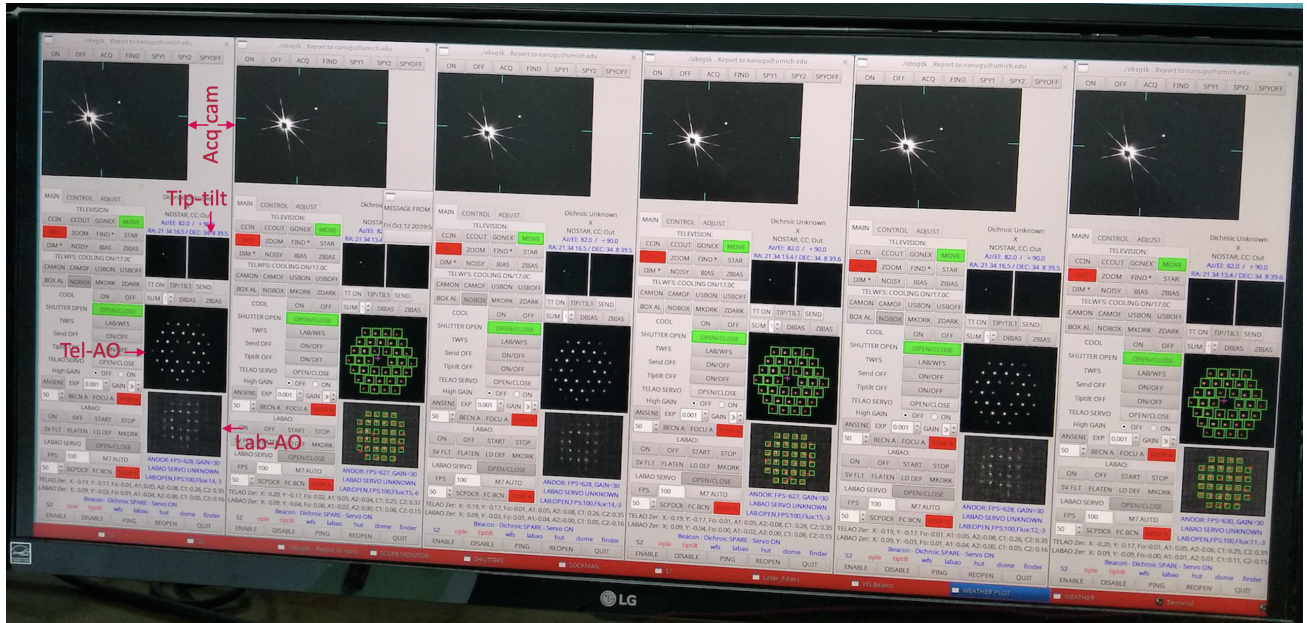


Figure 4. A photograph of the main observing GUI at the CHARA Array, obsgtk. Each obsgtk controls one telescope and has all the controls for the telescope and its acquisition camera, tip-tilt, Tel-AO, and Lab-AO, including the real-time displays of the acquisition camera and wavefront sensors of Tel-AO and Lab-AO. This GUI is optimized for screen space – all six GUIs fit in a single screen monitor, time-efficient usage, and stability by keeping only the required observing controls together. This photograph is taken with telescope beacon was ON.

3.3 Observational complexity of operating six Tel-AO + six Lab-AO

The adaptive optics systems software is built leveraging on the CHARA Array client/server architecture.¹ Servers publish the information, and appropriate clients subscribe to the servers to get the information. We do not have a central database system. The hardware (cameras, DMs, and other actuators) is controlled by the servers installed at the site of AO systems. We use GNU Tool Kit (GTK) Graphical User Interface (GUI) clients installed on the computers at the control room to send user configurations to the servers and monitor the real-time display of acquisition cameras and wavefront sensor cameras.

The control of six telescopes, six acquisition cameras, twelve adaptive optics systems, and six tip-tilt systems is challenging for an operator considering several GUIs. The GUIs of twelve adaptive optics systems take a lot of computer screen space and would require around six monitors. Requiring hands-on interaction with a large number of subsystem GUI's is not a practical solution for a telescope facility that must work with a single operator. A software solution is required that simplifies the control problem. This problem is approached with an integrated GUI for each telescope for saving screen space, operational efficiency, time-saving, and easy usability. We took critical real-time displays, buttons, and features from the engineering GUIs of different systems and put them into the integrated GUI. In the end, the GUIs of all the telescopes, acquisition cameras, adaptive optics systems, and tip-tilts systems are fit into a single computer display monitor, as shown in Figure 4.

The integrated GUI, `obsgtk`, connects and communicates with several servers including telescope (e.g., `S1`), acquisition camera (e.g., `S1_ACQ`), dome (e.g., `dome_S1`), motors server (e.g., `S1_HUT`), Tel-AO (e.g., `wfs_S1`) and Lab-AO (e.g., `LABAO_S1`). Where `S1` being the name of a telescope and names of other telescopes are `S2`, `W1`, `W2`, `E1` and `E2`. The display of real-time images from the cameras are built with GTK + XWindow system and they are fast and use very less CPU and memory usage.

3.4 Automatic alignment of Tel-AO and Lab-AO for beam drifts

The Lab-AO systems are connected to the Tel-AO systems using a metrology system. A dichroic at the telescope reflects some visible wavelengths of starlight into the Tel-AO WFS and also sends the beacon light into the Lab-AO WFS. It is very critical for the beacon light to follow the same path as the starlight.

An automatic alignment software tracks telescope pupil and focus drifts in both the Tel-AO and Lab-AO WFS that can be caused by beacon position drifts and by the temperature changes during the course of observing. These pupil and focus drifts are corrected with several actuators, including M1, M2, M7, and M10 mirrors of the telescope as the Tel-AO's alignment is strongly coupled to the alignment of the telescope itself. The beacon alignment is strongly coupled to the quality of the Coudé path alignment. The AO system has several automatic alignment controls, and a few are listed below:

- Align the focus of the WFS feed parabola.
- Align the beacon to the WFS.
- Focusing the telescope sending starlight to the WFS.
- Align beacon focus.
- Align of M7 of the telescope.
- Align of M10 of the telescope.

3.5 The Tel-AO performance

Figure 5 shows the performance of the Tel-AO for an integration time of 2ms. For this integration, the camera operates at a 440Hz measured frame rate and has a -3dB closed-loop bandwidth of 19Hz. For comparison, this is almost similar performance to the adaptive optics system of the Auxiliary Telescopes of the VLTI (NAOMI)²⁶ that runs at 500Hz and has -3dB closed-loop bandwidth of 18Hz.

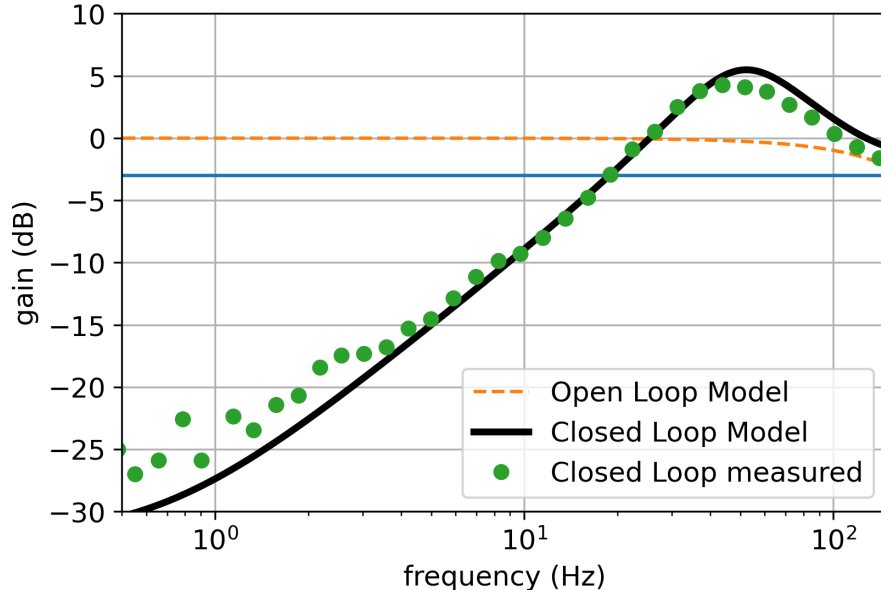


Figure 5. Rejection transfer function measured using the telescope beacon as the source of light. The green dotted line is the measured closed-loop transfer function. The dashed line is the modeled open-loop transfer function. The thick black line is the modeled closed-loop transfer function. This model uses the total delay time T_D is used. The green line cross the measured -3dB closed-loop bandwidth at frequency of 19Hz.

To verify the system performance, we have modeled the transfer function by putting the total delays of the control system, T_D (see Figure 5). The total cycle time is the sum of the integration (2ms) and frame-transfer and readout time (1.8ms) that is $T_C = 3.8\text{ms}$ for 2ms integration. The computational time for reading raw images from the instrument shared memory, computation of slopes, and computation of DM commands from slopes is $T_{RTC} = 0.7\text{ms}$. The total delay is $T_D = T_C + T_{RTC}$.

3.6 The Lab-AO performance

The Lab-AO systems have been used since 2014 to measure a good “default flat” of the sky close to the target star, and this has proved to be very helpful in coupling the light into the single-mode fibers used in many beam combiners.²⁷ We yet to measure the Tel-AO and Lab-AO’s final performance in terms of sensitivity due to the COVID-19 and 2020 Bobcat Fire, but these systems already show increased throughput more than a magnitude.

4. SUMMARY AND FUTURE PLANS

We here report the CHARA Array adaptive optics systems from the software perspective – highlighting operational complexity, solutions, and performance. An adaptive optics system’s success depends on a lot of “end-to-end” closed-loop testing with its calibration source and the on-sky. We have tested all the subsystems, including simultaneous operation of Tel-AO and Lab-AO since 2018 in various observing conditions. The Tel-AO’s -3dB closed-loop transfer function bandwidth is measured at 19Hz, and this performance is almost similar to NAOMI instrument,²⁶ which also uses the same model Andor 897 camera. The on-sky science observations with AOs are routine since the beginning of 2020. The on-sky tests are very promising, with more than a magnitude sensitivity improvement. We calculate more than 50% Strehl ratio achieved in the H and K-bands. These results push observations of faint young stellar object disks and active galactic nuclei, and other interesting systems. The AO also push the observations in worse seeing conditions, which were not possible without the adaptive optics system before. The sensitivity improvements will be enjoyed by beam combines operating in the H and K-bands, for instance, MIRC-X,¹³ CLASSIC/CLIMB²⁸ and upcoming MYSTIC.¹⁵

The adaptive optics systems are used not only for improving the throughput but also for other science cases:

- The Tel-AO and Lab-AO WFS pupil images can also be used to track the pupil between the telescope and the laboratory separated by many hundreds of meters of the optical path using starlight. This information is important for the estimation of accurate astrometry (e.g., MIRC-X astrometric mode²⁹) by computing pupil shifts projected on the telescope space³⁰ during the course of observing. The Tel-AO and Lab-AO images from the telemetry will be used to measure pupil shifts in the post-processing.
- The Telescope DMs will be used to take sky thermal backgrounds for the upcoming MYSTIC¹⁵ instrument by exploiting the large stroke of the ALPAO deformable mirrors.

We had to return two deformable mirrors to the ALPAO company for repairs. One for an upgrade and another to replace a bad actuator. They are expected to arrive in 2021 and will be installed once the COVID-19 situation is under control. During the first days of commissioning, the time taken to slew to a new target, acquisition, and locking all AO systems was almost double the slew time without the adaptive optics systems. However, since then, we have gained experience in our operations and reduced the total acquisition times. We are still learning and improving the better strategies for the interplay between the Tel-AO and Lab-AO systems and simplification of the operational aspects.

Our software is on the CHARA GitLab but private repository (<https://gitlab.chara.gsu.edu/chara>). If the reader is interested in accessing the software or discussing it, please feel free to contact the authors.

ACKNOWLEDGMENTS

This work is based upon observations obtained with the Georgia State University Center for High Angular Resolution Astronomy Array at Mount Wilson Observatory. The CHARA Array is supported by the National Science Foundation under Grant No. AST-1211929, AST-1411654, AST-1636624, and AST-1715788. Institutional support has been provided from the GSU College of Arts and Sciences and the GSU Office of the Vice President for Research and Economic Development.

REFERENCES

- [1] ten Brummelaar, T. A., McAlister, H. A., Ridgway, S. T., Bagnuolo, W. G., J., Turner, N. H., Sturmman, L., Sturmman, J., Berger, D. H., Ogden, C. E., Cadman, R., Hartkopf, W. I., Hopper, C. H., and Shure, M. A., “First Results from the CHARA Array. II. A Description of the Instrument,” *Astrophysical Journal* **628**, 453–465 (July 2005).
- [2] ten Brummelaar, T. A., Gies, D. G., McAlister, H. A., Ridgway, S. T., Sturmman, J., Sturmman, L., Schaefer, G. H., Turner, N. H., Farrington, C. D., Scott, N. J., Monnier, J. D., and Ireland, M. J., “An update on the CHARA array,” in [*Optical and Infrared Interferometry and Imaging V*], Malbet, F., Creech-Eakman, M. J., and Tuthill, P. G., eds., *Society of Photo-Optical Instrumentation Engineers (SPIE) Conference Series* **9907**, 990703 (Aug. 2016).
- [3] Schaefer, G. H. and et al., “Recent highlights from the CHARA Array,” in [*Optical and Infrared Interferometry and Imaging VII*], *Society of Photo-Optical Instrumentation Engineers (SPIE) Conference Series* **11446** (2020).
- [4] Monnier, J. D., Zhao, M., Pedretti, E., Thureau, N., Ireland, M., Muirhead, P., Berger, J. P., Millan-Gabet, R., Van Belle, G., ten Brummelaar, T., McAlister, H., Ridgway, S., Turner, N., Sturmman, L., Sturmman, J., and Berger, D., “Imaging the Surface of Altair,” *Science* **317**, 342 (July 2007).
- [5] Roettenbacher, R. M., Monnier, J. D., Korhonen, H., Aarnio, A. N., Baron, F., Che, X., Harmon, R. O., Kővári, Z., Kraus, S., Schaefer, G. H., Torres, G., Zhao, M., Ten Brummelaar, T. A., Sturmman, J., and Sturmman, L., “No Sun-like dynamo on the active star ζ Andromedae from starspot asymmetry,” *Nature* **533**, 217–220 (May 2016).
- [6] Kloppenborg, B., Stencel, R., Monnier, J. D., Schaefer, G., Zhao, M., Baron, F., McAlister, H., ten Brummelaar, T., Che, X., Farrington, C., Pedretti, E., Sallave-Goldfinger, P. J., Sturmman, J., Sturmman, L., Thureau, N., Turner, N., and Carroll, S. M., “Infrared images of the transiting disk in the ϵ Aurigae system,” *Nature* **464**, 870–872 (Apr. 2010).

- [7] Kraus, S., Kreplin, A., Young, A. K., Bate, M. R., Monnier, J. D., Harries, T. J., Avenhaus, H., Kluska, J., Laws, A. S. E., Rich, E. A., Willson, M., Aarnio, A. N., Adams, F. C., Andrews, S. M., Anugu, N., Bae, J., ten Brummelaar, T., Calvet, N., Curé, M., Davies, C. L., Ennis, J., Espillat, C., Gardner, T., Hartmann, L., Hinkley, S., Labdon, A., Lanthermann, C., LeBouquin, J.-B., Schaefer, G. H., Setterholm, B. R., Wilner, D., and Zhu, Z., “A triple-star system with a misaligned and warped circumstellar disk shaped by disk tearing,” *Science* **369**, 1233–1238 (Sept. 2020).
- [8] Schaefer, G. H., Brummelaar, T. T., Gies, D. R., Farrington, C. D., Kloppenborg, B., Chesneau, O., Monnier, J. D., Ridgway, S. T., Scott, N., Tallon-Bosc, I., McAlister, H. A., Boyajian, T., Maestro, V., Mourard, D., Meilland, A., Nardetto, N., Stee, P., Sturmman, J., Vargas, N., Baron, F., Ireland, M., Baines, E. K., Che, X., Jones, J., Richardson, N. D., Roettenbacher, R. M., Sturmman, L., Turner, N. H., Tuthill, P., van Belle, G., von Braun, K., Zavala, R. T., Banerjee, D. P. K., Ashok, N. M., Joshi, V., Becker, J., and Muirhead, P. S., “The expanding fireball of Nova Delphini 2013,” *Nature* **515**, 234–236 (Nov. 2014).
- [9] Boyajian, T. S., von Braun, K., van Belle, G., McAlister, H. A., ten Brummelaar, T. A., Kane, S. R., Muirhead, P. S., Jones, J., White, R., Schaefer, G., Ciardi, D., Henry, T., López-Morales, M., Ridgway, S., Gies, D., Jao, W.-C., Rojas-Ayala, B., Parks, J. R., Sturmman, L., Sturmman, J., Turner, N. H., Farrington, C., Goldfinger, P. J., and Berger, D. H., “Stellar Diameters and Temperatures. II. Main-sequence K- and M-stars,” *The Astrophysical Journal* **757**, 112 (Oct. 2012).
- [10] Sturmman, L., Sturmman, J., ten Brummelaar, T., and McAlister, H. A., “Nine-channel tip/tilt detector at the CHARA Array,” in [*Advances in Stellar Interferometry*], Monnier, J. D., Schöller, M., and Danchi, W. C., eds., *Society of Photo-Optical Instrumentation Engineers (SPIE) Conference Series* **6268**, 62683T (June 2006).
- [11] Shaklan, S. B. and Roddier, F., “Single-mode fiber optics in a long-baseline interferometer,” *Applied optics* **26**, 2159–2163 (June 1987).
- [12] Anugu, N., Le Bouquin, J.-B., Monnier, J. D., Kraus, S., Ennis, J., Lanthermann, C., Setterholm, B. R., Davies, C. L., ten Brummelaar, T., Haidar, M., Dubravec, V., and Peters, S., “MIRC-X/CHARA: sensitivity improvements with an ultra-low noise SAPHIRA detector,” in [*Proc. SPIE*], *Society of Photo-Optical Instrumentation Engineers (SPIE) Conference Series* **10701**, 1070124 (July 2018).
- [13] Anugu, N., Le Bouquin, J.-B., Monnier, J. D., Kraus, S., Setterholm, B. R., Labdon, A., Davies, C. L., Lanthermann, C., Gardner, T., Ennis, J., Johnson, K. J. C., Ten Brummelaar, T., Schaefer, G., and Sturmman, J., “MIRC-X: A Highly Sensitive Six-telescope Interferometric Imager at the CHARA Array,” *AJ* **160**, 158 (Oct. 2020).
- [14] Anugu, N., Le Bouquin, J.-B., Monnier, J. D., Kraus, S., Setterholm, B. R., Labdon, A., Davies, C. L., Lanthermann, C., Gardner, T., Ennis, J., Johnson, K. J. C., Ten Brummelaar, T., Schaefer, G., Sturmman, J., and Matt, A., “CHARA/MIRC-X - a high-sensitive six telescope interferometric imager concept, commissioning, and early science,” in [*Optical and Infrared Interferometry and Imaging VII*], *Society of Photo-Optical Instrumentation Engineers (SPIE) Conference Series* **11446** (2020).
- [15] Monnier, J. D., Le Bouquin, J.-B., Anugu, N., Kraus, S., Setterholm, B. R., Ennis, J., Lanthermann, C., Jocou, L., and ten Brummelaar, T., “MYSTIC: Michigan Young Star Imager at CHARA,” in [*Optical and Infrared Interferometry and Imaging VI*], *Society of Photo-Optical Instrumentation Engineers (SPIE) Conference Series* **10701**, 1070122 (July 2018).
- [16] Mourard, D., Bériot, P., Perraut, K., Clause, J.-M., Creevey, O., Martinod, M.-A., Meilland, A., Millour, F., and Nardetto, N., “SPICA, Stellar Parameters and Images with a Cophased Array: a 6T visible combiner for the CHARA array,” *Journal of the Optical Society of America A* **34**, A37 (May 2017).
- [17] Pannetier, C., Mourard, D., Bériot, P., Cassaing, F., Allouch, F., Anugu, N., Bailet, C., ten Brummelaar, T., Dejonghe, J., Gies, D., Jocou, L., Kraus, S., Lacour, S., Lagarde, S., LeBouquin, J., Lecron, D., Monnier, J., Nardetto, N., Patru, F., Perraut, K., Petrov, R., Rousseau, S., Stee, P., Sturmman, J., and Sturmman, L., “Progress of the CHARA/SPICA developments: Compensation of path length fluctuations and chromatism in the visible,” in [*Optical and Infrared Interferometry and Imaging VII*], *Society of Photo-Optical Instrumentation Engineers (SPIE) Conference Series* **11446** (2020).
- [18] Ruilier, C., “A study of degraded light coupling into single-mode fibers,” in [*Astronomical Interferometry*], Reasenberg, R. D., ed., *Society of Photo-Optical Instrumentation Engineers (SPIE) Conference Series* **3350**, 319–329 (July 1998).

- [19] ten Brummelaar, T. A., Sturmann, J., Sturmann, L., Anderson, M. D., Turner, N. H., Ireland, M. J., Monnier, J. D., Mourard, D., Ridgway, S. T., Gies, D. R., and Le Bouquin, J.-B., “The CHARA array adaptive optics program,” in [*Adaptive Optics Systems VI*], Close, L. M., Schreiber, L., and Schmidt, D., eds., *Society of Photo-Optical Instrumentation Engineers (SPIE) Conference Series* **10703**, 1070304 (July 2018).
- [20] ten Brummelaar, T., Che, X., McAlister, H. A., Ireland, M., Monnier, J. D., Mourard, D., Ridgway, S. T., sturmann, j., Sturmann, L., Turner, N. H., and Tuthill, P., “The CHARA Array Adaptive Optics Program,” in [*American Astronomical Society Meeting Abstracts #227*], *American Astronomical Society Meeting Abstracts* **227**, 427.02 (Jan. 2016).
- [21] Che, X., Sturmann, L., Monnier, J. D., ten Brummelaar, T. A., Sturmann, J., Ridgway, S. T., Ireland, M. J., Turner, N. H., and McAlister, H. A., “Optical and Mechanical Design of the CHARA Array Adaptive Optics,” *Journal of Astronomical Instrumentation* **2**, 1340007 (Dec. 2013).
- [22] ten Brummelaar, T. A., Sturmann, L., Sturmann, J., Ridgway, S. T., Monnier, J. D., Ireland, M. J., Che, X., McAlister, H. A., Turner, N. H., and Tuthill, P. G., “Adaptive optics for the CHARA array,” in [*Adaptive Optics Systems III*], Ellerbroek, B. L., Marchetti, E., and Véran, J.-P., eds., *Society of Photo-Optical Instrumentation Engineers (SPIE) Conference Series* **8447**, 84473I (July 2012).
- [23] ten Brummelaar, T., Che, X., McAlister, H., Ireland, M., Monnier, J., Mourard, D., Ridgway, S., Sturmann, J., Sturmann, L., Turner, N., and Tuthill, P., “CHARA array adaptive optics II: non-common-path correction and downstream optics,” in [*Adaptive Optics Systems IV*], Marchetti, E., Close, L. M., and Vran, J.-P., eds., *Society of Photo-Optical Instrumentation Engineers (SPIE) Conference Series* **9148**, 91484Q (Aug. 2014).
- [24] Che, X., Sturmann, L., Monnier, J. D., ten Brummelaar, T. A., Sturmann, J., Ridgway, S. T., Ireland, M. J., Turner, N. H., and McAlister, H. A., “The CHARA array adaptive optics I: common-path optical and mechanical design, and preliminary on-sky results,” in [*Adaptive Optics Systems IV*], Marchetti, E., Close, L. M., and Vran, J.-P., eds., *Society of Photo-Optical Instrumentation Engineers (SPIE) Conference Series* **9148**, 914830 (July 2014).
- [25] Anugu, N., Garcia, P. J., and Correia, C. M., “Peak-locking centroid bias in shack–hartmann wavefront sensing,” *Monthly Notices of the Royal Astronomical Society* **476**(1), 300–306 (2018).
- [26] Woillez, J., Abad, J. A., Abuter, R., Aller Carpentier, E., Alonso, J., Andolfato, L., Barriga, P., Berger, J. P., Beuzit, J. L., Bonnet, H., Bourdarot, G., Bourget, P., Brast, R., Caniguante, L., Cottalorda, E., Darré, P., Delabre, B., Delboulbé, A., Delplancke-Ströbele, F., Dembet, R., Donaldson, R., Dorn, R., Dupeyron, J., Dupuy, C., Egner, S., Eisenhauer, F., Fischer, G., Frank, C., Fuenteseca, E., Gitton, P., Gonté, F., Guerlet, T., Guieu, S., Gutierrez, P., Haguenaue, P., Haimerl, A., Haubois, X., Heritier, C., Huber, S., Hubin, N., Jolley, P., Jocu, L., Kirchbauer, J. P., Kolb, J., Kosmalski, J., Kreml, P., Le Bouquin, J. B., Le Louarn, M., Lilley, P., Lopez, B., Magnard, Y., Mclay, S., Meiland, A., Meister, A., Merand, A., Moulin, T., Pasquini, L., Paufigue, J., Percheron, I., Pettazzi, L., Pfuhl, O., Phan, D., Pirani, W., Quentin, J., Rakich, A., Ridings, R., Riedel, M., Reyes, J., Rochat, S., Santos Tomás, G., Schmid, C., Schuhler, N., Shcheketurov, P., Seidel, M., Soenke, C., Stadler, E., Stephan, C., Suárez, M., Todorovic, M., Valdes, G., Verinaud, C., Zins, G., and Zúñiga-Fernández, S., “NAOMI: the adaptive optics system of the Auxiliary Telescopes of the VLTI,” *A & A* **629**, A41 (Sept. 2019).
- [27] Martinod, M. A., Mourard, D., Bério, P., Perraut, K., Meiland, A., Bailet, C., Bresson, Y., ten Brummelaar, T., Clause, J. M., Dejonghe, J., Ireland, M., Millour, F., Monnier, J. D., Sturmann, J., Sturmann, L., and Tallon, M., “Fibered visible interferometry and adaptive optics: FRIEND at CHARA,” *A & A* **618**, A153 (Oct. 2018).
- [28] ten Brummelaar, T. A., Sturmann, J., Ridgway, S. T., Sturmann, L., Turner, N. H., McAlister, H. A., Farrington, C. D., Beckmann, U., Weigelt, G., and Shure, M., “The Classic/climb Beam Combiner at the CHARA Array,” *Journal of Astronomical Instrumentation* **2**, 1340004 (Dec. 2013).
- [29] Gardner, T., Monnier, J. D., Fekel, F. C., Schaefer, G., Johnson, K. J. C., Bouquin, J.-B. L., Kraus, S., Anugu, N., Setterholm, B. R., Labdon, A., Davies, C. L., Lanthermann, C., Ennis, J., Ireland, M., Kratter, K. M., Brummelaar, T. T., Sturmann, J., Sturmann, L., Farrington, C., Gies, D. R., Klement, R., and Adams, F. C., “Armada i: Triple companions detected in b-type binaries alpha del and nu gem,” *AJ* (Nov. 2020).

- [30] Anugu, N., Amorim, A., Gordo, P., Eisenhauer, F., Pfuhl, O., Haug, M., Wieprecht, E., Wiezorrek, E., Lima, J., Perrin, G., Brandner, W., Straubmeier, C., Le Bouquin, J. B., and Garcia, P. J. V., “Methods for multiple-telescope beam imaging and guiding in the near-infrared,” *MNRAS* **476**, 459–469 (May 2018).